Real-space visualization of quantum phase transitions by network topology

Shehtab Zaman and Wei-Cheng Lee[*]

Department of Physics, Applied Physics, and Astronomy, Binghamton University–State University of New York, Binghamton, New York 13902, USA

We demonstrate that with appropriate quantum correlation function, a real-space network model can be constructed to study the phase transitions in quantum systems. For a three-dimensional bosonic system, a single-particle density matrix is adopted to construct an adjacency matrix. We show that a Bose-Einstein condensate transition can be interpreted as a transition into a small-world network, which is accurately captured by a small-world coefficient. For a one-dimensional disordered system, using the electron diffusion operator to build the adjacency matrix, we find that Anderson localized states create many weakly linked subgraphs, which significantly reduces the clustering coefficient and lengthens the shortest path. We show that the crossover from delocalized to localized regimes as a function of the disorder strength can be identified as a loss of global connection, which is revealed by the small-world coefficient as well as other independent measures such as robustness, efficiency, and algebraic connectivity. Our results suggest that quantum phase transitions can be visualized in real space and characterized by network analysis with suitable choices of quantum correlation functions.

I. INTRODUCTION

Complex network models have been employed to investigate various real-world systems such as social networks, information systems, biological systems, and physical systems [1,2]. Generally speaking, the architecture and dynamics of complex networks could be represented by graphs containing nodes and links. A number of measures calculated from network models have been proposed to reveal the internal structures of graphs, which offers valuable insights for the real-world interacting systems of our interest. In the pioneering work done by Watts and Strogatz [3], the concept of the small-world network is introduced to describe systems whose nodes are highly clustered like regular lattices but have path lengths between nodes as small as random graphs. It has been shown that the small-world network has many advantages, such as fast information transmission, high synchronizability, etc., and many real-world systems such as human social groups, Internet world in cyberspace, and biological systems have been shown to exhibit small-world characteristics [4–9]. It is remarkable that all these radically different systems could be described by the same network model, regardless of the microscopic origins of the interactions that build up these systems.

Phase transitions in quantum systems have been one of the most important subjects in physics. By varying some physical parameters, the ground state could change abruptly so that the system could exhibit very distinct physical properties. In the field of network science, it has been shown that some network models could be mapped into certain quantum systems, and consequently the nature of the network properties could be understood using the same ideas developed in quantum physics. For example, the model proposed by Bianconi and Barabási [10] is shown to follow Bose statistics and even undergo Bose-Einstein condensation. Fermi-Dirac statistics is shown to emerge in growing Cayley trees with thermal noise [11], and a class of generalized statistics for networks has been proposed [12]. While there is growing interest in applying ideas from quantum systems to explore the relations in networks [13–19], the possibility of using network science to explore the nature of phase transitions in quantum systems attracts much less attention [20–22]. The key issue is the absence of an intuitive way to define nodes and links representing phase transitions in quantum systems. Recently, Chou [23] demonstrated that the topological phase transition in a *p*-wave superconductor can be characterized by network science using a pairing amplitude to construct an adjacency matrix. This analysis, however, is based on the mean-field Hamiltonian that assumes the existence of superconductivity, thus it cannot be used to describe general cases of phase transition in quantum systems.

In this paper, we demonstrate that the phase transitions in quantum systems can be studied by network models with suitable quantum correlation functions defined in real space. We test this idea in two cases that can be solved exactly. For a three-dimensional noninteracting bosonic system, a single-particle density matrix is exploited to define the adjacency matrix for the weighted network. We show that the Bose-Einstein condensate can be viewed as a small world in our network model due to the presence of off-diagonal long-range order (ODLRO) [24]. For a one-dimensional disordered system, a weighted network is constructed using an electron diffusion operator [25]. We find that Anderson localized states create many weakly linked subgraphs in our network model, which greatly reduce the clustering coefficient and lengthen

the shortest path. We show that the crossover from delocalized to localized regimes with varying disorder strength can be reflected by a loss of global connection in the corresponding graphs, which can be clearly seen in the small-world coefficient as well as other independent network measures such as robustness, efficiency, and algebraic connectivity. Our results suggest that quantum phase transitions can be visualized in real space and characterized by network topology with suitable quantum correlation functions.

II. BOSE-EINSTEIN CONDENSATE IN A NONINTERACTING THREE-DIMENSIONAL BOSONIC SYSTEM

Consider a three-dimensional free boson system with fixed particle density n. The Hamiltonian can be written as

$$H = \int d\vec{r}\, \hat{\psi}^\dagger(\vec{r})\left(\frac{\hbar^2 \nabla^2}{2m} - \mu\right)\hat{\psi}(\vec{r}), \tag{1}$$

where $\hat{\psi}^\dagger(\vec{r})$ $[\hat{\psi}(\vec{r})]$ creates (annihilates) a boson at position $\vec{r}$. Introducing the Fourier transformation of $\hat{b}_{\vec{k}} = \frac{1}{\sqrt{V}}\int d\vec{r}\, e^{-i\vec{k}\cdot\vec{r}}\hat{\psi}(\vec{r})$, we can diagonalize the Hamiltonian as

$$H = \int \frac{d\vec{k}}{(2\pi)^3}[E(\vec{k}) - \mu]\hat{b}_{\vec{k}}^\dagger \hat{b}_{\vec{k}}, \tag{2}$$

where $E(\vec{k}) = \frac{\hbar^2 k^2}{2m}$, and the particle density n can be evaluated by

$$n = n_0 + n_e,$$
$$n_e = \frac{1}{(2\pi)^3}\int \frac{d\vec{k}}{e^{\beta[E(\vec{k})-\mu]} - 1}. \tag{3}$$

n_0 is the particle density occupying the ground state, while n_e is the particle density occupying all other states. The Bose-Einstein condensate (BEC) is identified by μ being equal to the ground-state energy and the emergence of off-diagonal long-range order (ODLRO) ($n_0 \neq 0$) [24], which occurs at a temperature below the critical temperature T_c of

$$k_B T_c = 4\pi \frac{\hbar^2}{2m}\left[\frac{n}{\zeta(3/2)}\right]^{\frac{2}{3}}. \tag{4}$$

$\zeta(s)$ is the Riemann zeta function.

Our goal is to build a real-space network model to capture the BEC transition. A natural choice is the single-particle density matrix defined as

$$\rho_{ij} \equiv \langle \hat{\psi}^\dagger(\vec{r}_i)\hat{\psi}(\vec{r}_j)\rangle = n_0 + f(\vec{r}_i - \vec{r}_j), \tag{5}$$

where

$$f(\vec{r}_i - \vec{r}_j) \equiv \int d\vec{k}\, \frac{e^{-i\vec{k}\cdot(\vec{r}_i-\vec{r}_j)}}{e^{\beta[E(\vec{k})-\mu]} - 1}. \tag{6}$$

Clearly, $f(\vec{r}_i - \vec{r}_j)$ goes to 0 as $|\vec{r}_i - \vec{r}_j| \to \infty$. In general, ρ_{ij} describes the probability of a boson hopping from $\vec{r}_j$ to $\vec{r}_i$, which serves as a good quantity to represent the "link" between different positions. Here we choose N points along the x direction with equal spacing of $l_c = \frac{1}{\sqrt{4\pi}}(\frac{\zeta(3/2)}{n})^{1/3}$. In other words, the position of the ith point is $\vec{r}_i = (il_c, 0, 0)$, where $i = 1, 2, \ldots, N$. We emphasize that the system is still

three-dimensional, and we just choose points along the x direction. Different choices of the set of points might give different values for the network measures, but the behavior as a function of temperature will be exactly the same. Now we can construct a network model with these N points being the nodes, and the adjacency matrix can be constructed based on a single-particle density matrix as

$$A_{ij} = 0, \quad i = j,$$
$$= \frac{|\rho_{ij}|}{\max(|\rho_{ij}|)}, \quad i \neq j. \tag{7}$$

The graph built by Eq. (7) has weighted links bounded within [0,1]. For the network properties, we have used $N = 50$ in all the calculations presented below.

We start from the local clustering coefficient that determines the connectivity of a given node in the graph. Following Ref. [26], we define the local clustering coefficient of the ith node as

$$C_i = \frac{1}{k_i(k_i - 1)}\sum_{j,k\in\{N_i\}} A_{jk}, \tag{8}$$

where $\{N_i\}$ is the set of neighboring nodes around the ith node, and k_i is the number of nodes in $\{N_i\}$. In an unweighted binary graph, $\{N_i\}$ is defined as the set of nodes j with $A_{ij} = 1$. Since our graph is a complete graph with weighted links, $\{N_i\}$ should just be the set of all the nodes other than i, which means $k_i = N - 1$ for every node. Equation (8) can naturally reproduce the clustering coefficient for an unweighted binary graph proposed in Ref. [3]. It is noted that this definition places more emphasis on the connections between neighboring nodes around the ith node without input from direct links to the ith node, which is different from another popular definition [23,27] of

$$C_i^O = \frac{1}{k_i(k_i - 1)}\sum_{j,k\in\{N_i\}} (A_{ij}A_{jk}A_{ki})^{1/3}. \tag{9}$$

C_i^O counts the number of triangles attached to the ith node with an effective intensity of $(A_{ij}A_{jk}A_{ki})^{1/3}$, and consequently the direct links to the ith node are as important as the links between its neighbors. Nevertheless, we find that general trends of the network properties are the same regardless of the choice of definition for the clustering coefficient. To measure the clustering of the entire graph G, we can compute the average clustering coefficient as

$$C(G) = \frac{1}{N}\sum_i C_i. \tag{10}$$

Note that in our definition, $0 \leqslant C(G) \leqslant 1$ and $C(G) = 1$ only occurs in a complete graph with $A_{ij} = 1$ for every $i \neq j$.

Another important quantity in the network science is the shortest path between two nodes, which posts a subtle issue using the adjacency matrix A_{ij} defined in Eq. (7). In the network theory, if A_{ij} is the weighted link between the ith and jth nodes, its value is usually expected to be proportional to the "distance" between these two nodes. This is, however, in contradiction to the meaning of the single-particle density matrix, which is proportional to the probability of a boson hopping from $\vec{r}_i$ to $\vec{r}_j$. In other words, in our graph, the larger A_{ij} is, the
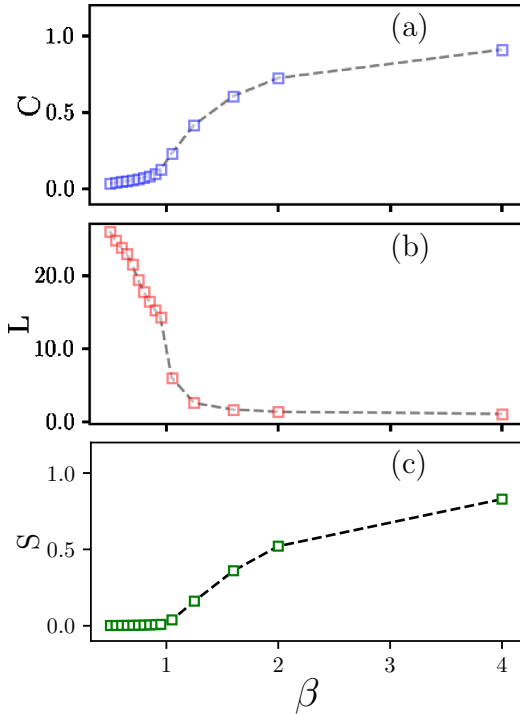
FIG. 1. (a) The average clustering coefficient, (b) average shortest path, and (c) small-world coefficient of the three-dimensional noninteracting boson system as a function of the normalized Boltzmann factor defined as $\beta = 1/t$, $t = T/T_c$.

shorter the "distance" between $\vec{r}_i$ and $\vec{r}_j$ should be. As a result, we follow Ref. [23] to use the "inverse" of the adjacency matrix A_{ij} to represent the "direct" distance between nodes i and j, denoted as $D_{ij} = 1/A_{ij}$. The shortest path between nodes i and j, namely d_{ij}, is defined as the minimal length between i and j on the matrix of D_{ij}, which can be found by the Dijkstra shortest path algorithm [28]. The global path length feature of the entire graph G can be revealed by averaging the shortest path

$$L(G) = \frac{1}{N(N-1)} \sum_{i \neq j \in G} d_{ij}. \tag{11}$$

Figure 1 presents $C(G)$ and $L(G)$ as a function of normalized Boltzmann factor $\beta = 1/t$ with $t = T/T_c$. It can be seen

clearly that as the system enters the BEC region from the normal state ($\beta < 1$), $C(G)$ increases and $L(G)$ decreases abruptly at $\beta = 1$, exhibiting the BEC transition. The kink at $\beta = 1$ associated with the BEC transition can be further amplified in the small-world coefficient defined as

$$S(G) = \frac{C(G)}{L(G)}, \tag{12}$$

which is shown in Fig. 1(c).

These results can be well understood by the existence of ODLRO given in Eq. (5). In the normal state ($\beta > 1$), $n_0 = 0$ and $f(\vec{r}_i - \vec{r}_j)$ goes to zero as $|\vec{r}_i - \vec{r}_j| \to \infty$. Consequently, many elements in the adjacency matrix are very small, and the normal state network tends to have a small $C(G)$ and long $L(G)$. In the BEC state ($\beta < 1$), every element in the adjacency matrix has the same order of magnitude due to the ODLRO ($n_0 \neq 0$), and the BEC network naturally has a large $C(G)$ and short $L(G)$, which are the key properties necessary for the small-world network.

To visualize the network constructed from Eq. (7), we draw the force-directed graphs obtained by the Kamada-Kawai cost function with the code developed by NetworkX [29]. In the force-directed graphs, repulsive interactions similar to the electrical Coulomb interaction are introduced among every pair of nodes, and an attractive interaction between two nodes resembling the spring force is added with a spring constant depending on the value of A_{ij}. The balance of these forces determines the positions of nodes in a two-dimensional plane, which is shown in Fig. 2. The change of the graph topology can be seen directly as β varies across the BEC transition. Compared to the graphs in the normal state, the distance between nodes is much more equal in the BEC graph [Fig. 2(d)], which is a clear signature for the small-world network. Based on the above analysis, we conclude that the BEC transition corresponds to the transition into a small-world network in the graph representation.

III. ANDERSON LOCALIZATION IN 1D FERMIONIC SYSTEMS

In this section, we employ the same idea to explore the properties of the real-space network representing the disordered fermionic system. For a proof of concept, we consider a one-dimensional periodic fermionic system with a
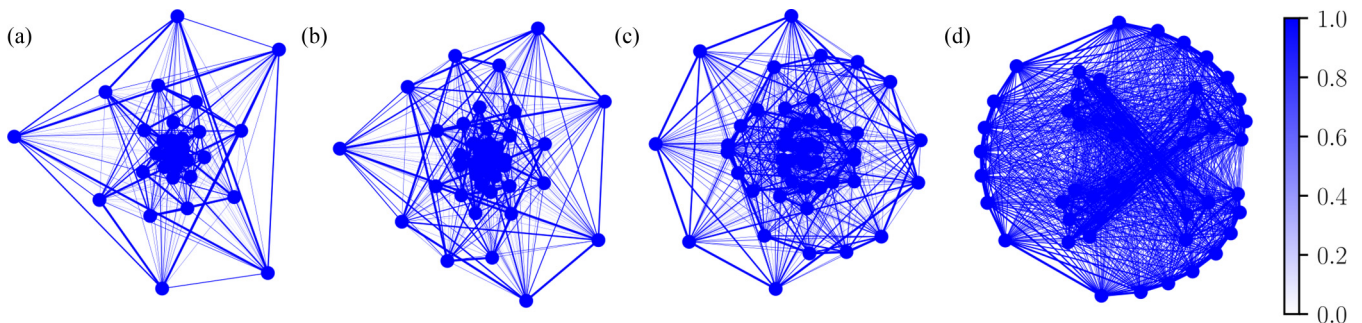

FIG. 2. The force-directed graphs of the network model using the adjacency matrix defined in Eq. (7) for the three-dimensional noninteracting boson system as a function of normalized Boltzmann factor defined as $\beta = 1/t$, $t = T/T_c$ for (a) $\beta = 0.85$, (b) $\beta = 0.89$, (c) $\beta = 0.94$, and (d) $\beta = 1.04$.
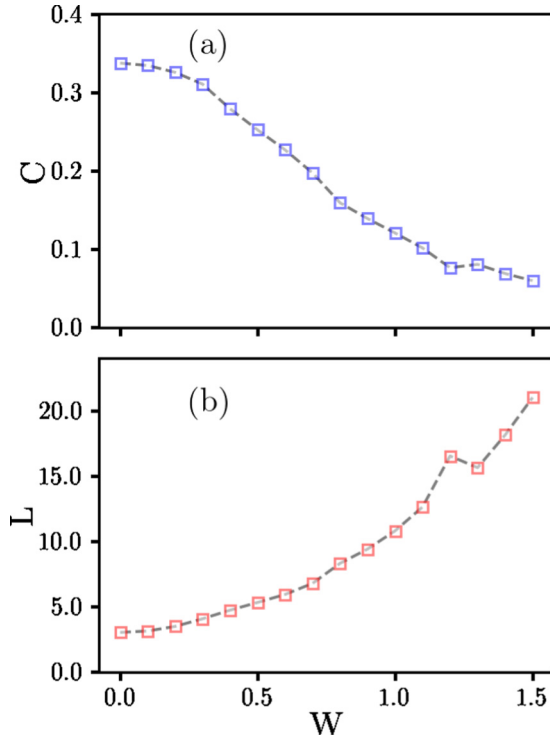
FIG. 3. (a) The average clustering coefficient and (b) the average shortest path for the graph representing a 1D disordered system as a function of disorder strength W.
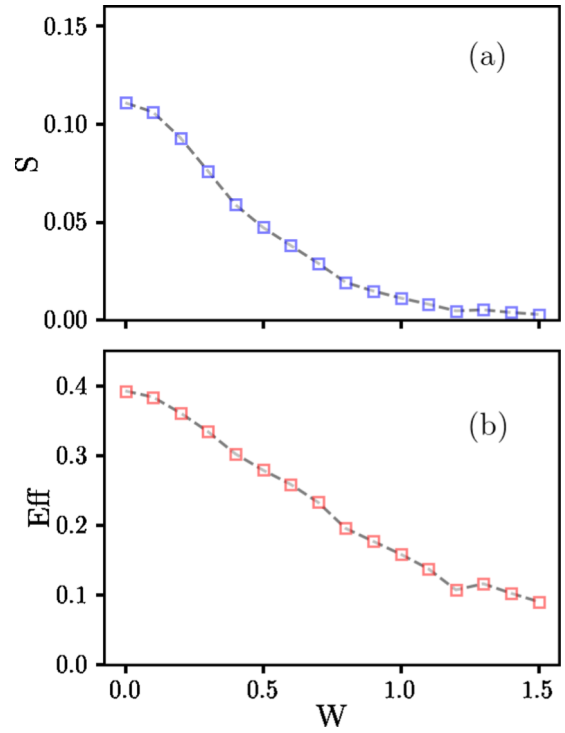

FIG. 4. (a) The small-world coefficient and (b) the efficiency for the graph representing a 1D disordered system as a function of disorder strength W.

Hamiltonian written as [30]

$$\hat{H} = -t \sum_{\langle i,j \rangle} \hat{c}_i^\dagger \hat{c}_j + \sum_i [W\epsilon_i - \mu]\hat{c}_i^\dagger \hat{c}_i, \quad (13)$$

where $\hat{c}^{\dagger i}$ ($\hat{c}_j$) creates (annihilates) a fermion at site i, t is the nearest-neighbor hopping integral, W is the disorder strength, μ is the chemical potential, and ϵ_i is a random number bounded between $[-\frac{1}{2}, \frac{1}{2}]$. We set $t = 1$ in the following calculations.

To construct the adjacency matrix, we use the diffusion operator [25] defined as

$$\Pi(i, j; \omega) \equiv \left\langle G_{ij}^R(\omega/2) G_{ji}^A(\omega/2) \right\rangle_{\text{dis}}. \quad (14)$$

Note that $\langle \cdots \rangle_{\text{dis}}$ denotes the average over different disorder configurations, and $G_{ij}^{R,A}(\omega)$ are the retarded and the advanced Green's functions between sites i and j,

$$G_{ij}^{R,A}(\omega) = \langle i|[(\omega \pm i\eta)\hat{I} - \hat{H}]^{-1}|j\rangle. \quad (15)$$

$\Pi(i, j; \omega = 0)$ is a real and positive quantity that can be interpreted as the probability of an electron diffusing between sites i and j and is consequently a useful quantity to detect the degree of localization in a disordered system [25]. As a result, we set up the adjacency matrix as

$$\hat{A}_{ij} = \frac{\Pi(i, j; 0)}{\text{Max}(\Pi(i, j; 0))}. \quad (16)$$

By symmetry, $\hat{A}_{ij} = \hat{A}_{ji}$ and we have transformed the 1D disordered system to a network model with undirected but weighted links. We can therefore use the same definitions of the clustering coefficient, the shortest path, and the small-

world coefficient introduced in the preceding section. We solve the model Hamiltonian given in Eq. (13) with 500 sites. We fix the chemical potential to be $\mu = 0$ and study the evolution of the graph as a function of the disorder strength W. For each disorder strength, we obtain $\Pi(i, j; 0)$ by averaging over 5000 different disorder configurations.

The average clustering coefficient and the average shortest path calculated based on the adjacency matrix in Eq. (16) are presented in Fig. 3 as a function of the disorder strength W. Clearly, the clustering coefficient C decreases as the disorder gets stronger, which can be understood by the nature of localization. Because of the Anderson localized states, electrons are more likely trapped in localized states near particular sites as the disorder strength gets stronger. In the network model constructed from Eq. (16), the reduction of the clustering coefficient with the increase of W is attributed to many weakly connected subgraphs resulting from localized states. Moreover, since the probability of electron hopping between different localized regions is generally small, the global average shortest path is expected to increase as a function of W, which is clearly shown in Fig. 3(b).

We shall mention that because a one-dimensional system is always in the localized regime in the presence of any disorder strength, we would not see a sharp transition as seen in the case of BEC. However, since we consider a finite-size system of 500 sites, we do see a crossover into a regime in which the localization length of every single-particle eigenstate is shorter than the system size. The critical disorder strength ($W_c \sim 1.2t$) for this crossover can be better characterized in the small-world coefficient plotted in Fig. 4(a). An intriguing feature in Fig. 4(a) is that the small-world coefficient
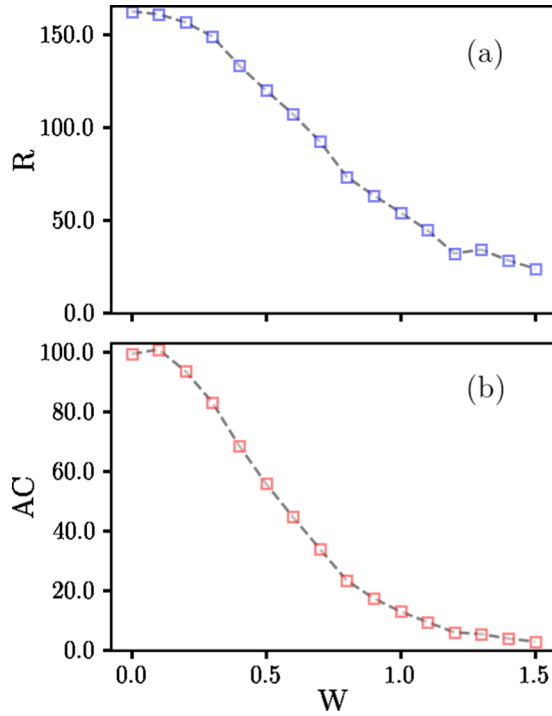
FIG. 5. (a) The robustness R and (b) the algebraic connectivity for the graph representing a 1D disordered system as a function of disorder strength W.

FIG. 6. The force-directed graphs for the 1D disordered system in (a) delocalized ($W = 0.5$) and (b) localized ($W = 1.5$) regimes. For the best quality, we only plot 50 out of 500 nodes so that the distances between nodes can be clearly seen.

becomes almost zero as $W > W_c$. This feature indicates that the system is no longer globally connected in the strong disorder limit, consistent with the fact that all the single-particle eigenstates have a localization length shorter than the system size, and consequently the electron diffusion is exponentially suppressed for any state.

We can further study the loss of global connection using other network measures. For example, the reciprocal shortest distance matrix is used in calculating graph invariants such as the Harary index [31,32], which has been employed to measure the compactness of molecular structures. A measure similar to the Harary index introduced in Ref. [33] has been exploited to indicate the efficiency of the graph, which is defined as the average of the inverse of the shortest path,

$$\text{Eff}(G) = \frac{1}{N(N-1)} \sum_{i \neq j \in G} \frac{1}{d_{ij}}. \tag{17}$$

Higher $\text{Eff}(G)$ corresponds to the increased ability of each node in the graph to disperse information simultaneously. We plot $\text{Eff}(G)$ as a function of W in Fig. 4(b), which demonstrates the increased difficulty in transferring information between sites in the strong disorder regime. Another quantity to analyze is the robustness R defined as [23,34–37]

$$R(G) = \ln\left(\frac{1}{N} \sum_i e^{\lambda_i}\right), \tag{18}$$

where $\{\lambda_i\}$ is the set of eigenvalues of the adjacency matrix $\hat{A}_{ij}$. R can be understood as a measure for the ability of the network to withstand nodes being removed without the global network features being affected. Generally speaking, a highly
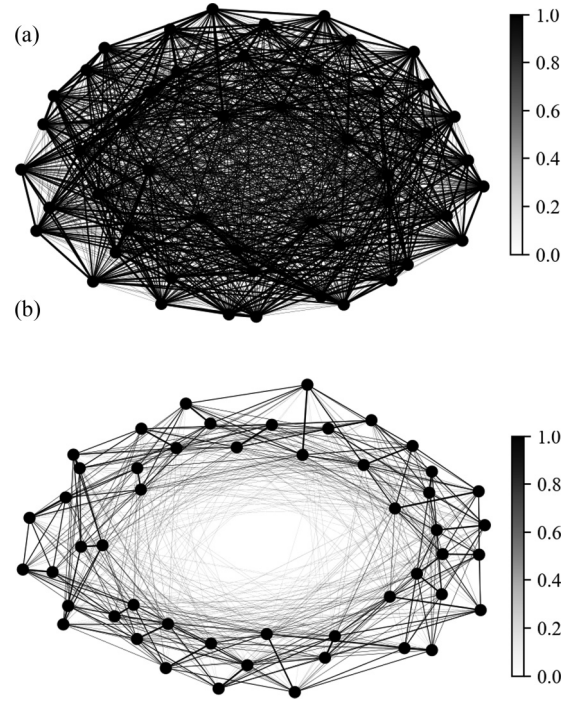
and globally connected graph tends to have a large value of R, meaning that removing a few nodes from the graph would not change the global properties of the graph significantly. The robustness R as a function of W is shown in Fig. 5(a). It can be seen that R goes to zero in the strong disorder regime, which can again be attributed to the loss of the global connection. In the strong disorder regime, there are many weakly linked subgraphs due to the localized states. As a result, removing a few nodes could disconnect completely the links between some subgraphs, and the connections between these affected subgraphs could be completely lost, which explains the vanishing value of R.

Lastly, we analyze the algebraic connectivity proposed by Fiedler [38], which is another gauge of the connectedness of a graph [39]. To obtain the algebraic connectivity, we introduce the degree matrix as

$$K_{ij} = 0, i \neq j,$$
$$= \sum_k A_{ik}, i = j. \tag{19}$$

The Laplacian matrix of the graph can therefore be constructed by

$$\hat{L} = \hat{K} - \hat{A}, \tag{20}$$

It can be shown that the smallest eigenvalue of $\hat{L}$ is always zero for any graph, which corresponds to the eigenvector of $(1, 1, 1, \dots)^T$. The second smallest eigenvalue, identified as the algebraic connectivity, is nonzero if and only if the graph is connected, and its value is proportional to the degree of the connectedness in a graph [39,40]. The algebraic connectivity

for the graph representing the disorder system is plotted in Fig. 5(b), which shows the same trends as the small-world coefficient, the robustness, and the efficiency.

To directly visualize the subgraphs in our network, we draw the force-directed graphs [29] in Fig. 6. In the delocalized regime [Fig. 6(a) for $W = 0.5$], nodes are more evenly distributed, indicating no tendency to form subgraphs. On the other hand, in the localized regime nodes tend to stay closer to particular neighbors, and consequently a lot of subgraphs can be observed directly in the plot [Fig. 6(b) for $W = 1.5$].

IV. CONCLUSIONS

In this paper, we have studied two cases of phase transitions in quantum systems using real-space network models. The key step is to choose a suitable quantum correlation function to construct the adjacency matrix, and the natural choice is the one encoding the "probability" of quantum particles moving from one place to another in real space. For a three-dimensional bosonic system we have chosen a single-particle density matrix, while for a one-dimensional disordered system we have chosen an electron diffusion operator. We have shown that phase transitions in these model systems can be accurately captured by a number of network measures, which allows us to visualize the quantum phase transitions in real space in terms of network science. For example, the clustering coefficient measures the tendency of the neighbors around a node to connect, and the shortest path determines how fast information can travel from one node to another. In the Bose-Einstein condensate (BEC), the off-diagonal long-range order provides global links between every node in the graph. As a result, the clustering coefficient increases and the shortest path decreases dramatically as the system undergoes the BEC transition, and in our network model the BEC transition can be characterized as a transition into a small-world network. For the one-dimensional disordered system, because of Anderson localized states, our network has many weakly linked subgraphs that greatly reduce the clustering coefficient and lengthen the shortest path. We have shown that the crossover from a delocalized to a localized regime as a function of disorder strength can be well captured by the small-world coefficient as well as other independent measures such as robustness, efficiency, and algebraic connectivity.

Our formalism can be easily generalized to study quantum phase transitions in other systems. For example, quantum phase transitions in interacting fermionic systems can be analyzed by network models constructed by two-particle density matrices [24] such as the spin-spin correlation function for magnetism, the Cooper-pairing correlation function for superconductivity, and the density-density correlation function for charge ordering. A similar idea was presented in Refs. [41,42], in which a quantum mutual information matrix constructed from one and two point correlators is introduced to study quantum phase transitions in the Ising spin chain. Our results demonstrate that quantum phase transitions can be visualized in real space and characterized by network topology with suitable quantum correlation functions.

[1] M. Girvan and M. E. Newman, Proc. Natl. Acad. Sci. USA **99**, 7821 (2002).

[2] Y. Braiman, J. F. Lindner, and W. L. Ditto, Nature (London) **378**, 465 (1995).

[3] S. S. Duncan Watts, Nature (London) **393**, 440 (1998).

[4] J. M. Montoya and R. V. Solé, J. Theor. Biol. **214**, 405 (2002).

[5] R. Guimera, L. Danon, A. Diaz-Guilera, F. Giralt, and A. Arenas, Phys. Rev. E **68**, 065103(R) (2003).

[6] H. Jeong, S. P. Mason, A.-L. Barabási, and Z. N. Oltvai, Nature (London) **411**, 41 (2001).

[7] E. Bullmore and O. Sporns, Nat. Rev. Neurosci. **10**, 186 (2009).

[8] D. S. Bassett, E. Bullmore, B. A. Verchinski, V. S. Mattay, D. R. Weinberger, and A. Meyer-Lindenberg, J. Neurosci. **28**, 9239 (2008).

[9] S. Achard and E. Bullmore, PLoS Comput. Biol. **3**, e17 (2007).

[10] G. Bianconi and A.-L. Barabási, Phys. Rev. Lett. **86**, 5632 (2001).

[11] G. Bianconi, Phys. Rev. E **66**, 036116 (2002).

[12] D. Garlaschelli and M. I. Loffredo, Phys. Rev. Lett. **102**, 038701 (2009).

[13] C.-P. Zhu and S.-J. Xiong, Phys. Rev. B **62**, 14780 (2000).

[14] E. López, S. V. Buldyrev, S. Havlin, and H. E. Stanley, Phys. Rev. Lett. **94**, 248701 (2005).

[15] M. Sade, T. Kalisky, S. Havlin, and R. Berkovits, Phys. Rev. E **72**, 066123 (2005).

[16] L. Jahnke, J. W. Kantelhardt, R. Berkovits, and S. Havlin, Phys. Rev. Lett. **101**, 175702 (2008).

[17] G. Bianconi, C. Rahmede, and Z. Wu, Phys. Rev. E **92**, 022815 (2015).

[18] G. Bianconi, Europhys. Lett. **111**, 56001 (2015).

[19] J.-L. Guo, Q. Suo, A.-Z. Shen, and J. Forrest, Sci. Rep. **6**, 33651 (2016).

[20] G. Bianconi, Phys. Rev. E **85**, 061113 (2012).

[21] A. Halu, L. Ferretti, A. Vezzani, and G. Bianconi, Europhys. Lett. **99**, 18001 (2012).

[22] A. Halu, S. Garnerone, A. Vezzani, and G. Bianconi, Phys. Rev. E **87**, 022104 (2013).

[23] C.-P. Chou, Sci. Rep. **4**, 7526 (2014).

[24] C. N. Yang, Rev. Mod. Phys. **34**, 694 (1962).

[25] F. Evers and A. D. Mirlin, Rev. Mod. Phys. **80**, 1355 (2008).

[26] L. López-Fernández, G. Robles, J. M. Gonzalez-Barahona, and I. Herraiz, Int. J. Inf. Technol. Web Eng. (IJITWE) **1**, 27 (2006).

[27] J.-P. Onnela, J. Saramäki, J. Kertész, and K. Kaski, Phys. Rev. E **71**, 065103(R) (2005).

[28] E. W. Dijkstra, Numer. Math. **1**, 269 (1959).

[29] A. A. Hagberg, D. A. Schult, and P. J. Swart, Exploring network structure, dynamics, and function using NetworkX, in *Proceedings of the 7th Python in Science Conference (SciPy2008)*, edited by G. Varoquaux, T. Vaught, and J. Millman (Pasadena, CA USA, 2008), pp. 11–15.

[30] P. Anderson, Phys. Rev. **109**, 1492 (1958).

[31] D. Plavšić, S. Nikolić, N. Trinajstić, and Z. Mihalić, J. Math. Chem. **12**, 235 (1993).

[32] O. Ivanciuc, T. S. Balaban, and A. T. Balaban, J. Math. Chem. **12**, 309 (1993).

[33] V. Latora and M. Marchiori, Phys. Rev. Lett. **87**, 198701 (2001).

[34] E. Estrada, Chem. Phys. Lett. **319**, 713 (2000).

[35] E. Estrada and J. A. Rodríguez-Velázquez, Phys. Rev. E **71**, 056103 (2005).

[36] E. Estrada and N. Hatano, Chem. Phys. Lett. **439**, 247 (2007).

[37] E. Estrada, N. Hatano, and M. Benzi, Phys. Rep. **514**, 89 (2012).

[38] M. Fiedler, Czech. Math. J. **23**, 298 (1973).

[39] J. Wu, M. Barahona, Y.-J. Tan, and H.-Z. Deng, IEEE Trans. Syst., Man, Cybern.-Pt. A **41**, 1244 (2011).

[40] N. M. M. De Abreu, Linear Alg. Appl. **423**, 53 (2007).

[41] M. A. Valdez, D. Jaschke, D. L. Vargas, and L. D. Carr, Phys. Rev. Lett. **119**, 225301 (2017).

[42] B. Sundar, M. A. Valdez, L. D. Carr, and K. R. A. Hazzard, Phys. Rev. A **97**, 052320 (2018).